Hindawi
Shock and Vibration
Volume 2020, Article ID 8015465, 14 pages
https://doi.org/10.1155/2020/8015465

Research Article

Development and Verification of the Diagnostic Model of the Sieving Screen

Pavlo Krot,[1] Radoslaw Zimroz,[1] Anna Michalak,[1] Jacek Wodecki,[1] Szymon Ogonowski,[2] Michal Drozda,[3] and Marek Jach[3]

[1]*Faculty of Geoengineering, Mining and Geology, Wroclaw University of Science and Technology, Wroclaw 50-421, Poland*
[2]*AMEplus Sp. z o.o., Gliwice 44-121, Poland*
[3]*KGHM Polska Miedz SA, Oddzial Zaklady Wzbogacania Rud, Kopalniana 1, 5 Polkowice 9-101, Poland*

Correspondence should be addressed to Radoslaw Zimroz; radoslaw.zimroz@pwr.edu.pl

Received 21 February 2020; Revised 1 May 2020; Accepted 27 May 2020; Published 18 June 2020

Academic Editor: Anil Kumar

The minerals processing enterprises are widely using vibrating machines to separate different fractions of materials. Sieving efficiency is greatly dependent on particle trajectories, or orbit, of periodical motion over the sieving decks. A screening process is very dependable on design parameters such as the vibrator power, synchronisation of their drives, and oscillation frequency as well as the stiffness of supporting springs. Deterioration of supporting springs (stiffness reduction and cracks) due to cyclic loading and fatigue is difficult to determine by the visual inspection, static loading tests, or nondestructive testing techniques. Vibration monitoring systems of different vendors are analysed where vibration sensors usually installed on the bearings of vibrators are as well used for supporting springs diagnostics. However, strong cyclic components from the unbalanced exciters and stochastic disturbances from the input stream and vibrating pieces of the material make analysis a not trivial task. The considered vibrating screen is investigated on the 6-DOF (degree-of-freedom) dynamical model to reflect all linear and rotational components of spatial motion. Besides the main periodic motion, the model accounts for stochastic alpha-stable distributed impacts from the material. Instead, the Gaussian normal distribution is considered for the position of equivalent force application point. Supporting springs are represented by the bilinear stiffness characteristics. Specific features of vibration signals (angle of orbit inclination, natural frequency change, harmonics of natural frequency, and phase space plots) are analysed to recognise the weak nonlinear features of a system under conditions of small stiffness changes in springs. The extensive measurements are conducted on the industrial vibrating screen, and the dynamic model is verified by the measurement data. Recommendations are given on failure diagnostics of springs in the industrial vibrating screens.

1. Introduction

A wide variety of vibrating screens are engaged in the raw material processing and aggregate industries. These vibrating machines are involved in the separation by the fractions of ore, coal, and other bulk materials. Having a wide range of power, design, and number of decks, sieving screens can process from 10 to over 1000 tons of material per hour.

Cyclic excitation of the screen decks can be realised by the unbalanced rotating shafts, hydraulic cylinders, or electromagnetic actuators. Using decks and particles motion criteria, screens are categorised into circular, elliptical, or linear types. Some other types of trajectories or vibration fields can be provided. To increase the overall productivity and final quality, several decks can be used.

The typical vibrating screen comprises the body and side panels connected by reinforcing beams, multiple sieving decks, and helical springs (see Figure 1(a)). All parts of the screen experience a significant level of wear; therefore, instead of welded joints, huck bolts are implemented.

Sieving ore is fed to the screen by using the belt conveyor having a certain linear speed. The upper deck of the screen is usually designed as grizzly bars, which provide scalping of

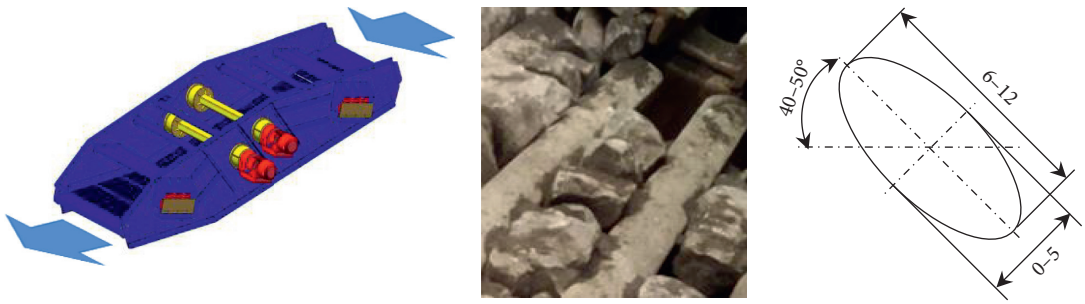

(a) (b) (c)

Figure 1: Vibrating screen (mifama.com.pl) (a); blinding with a near mesh size material (b); orbit of motion (c).

the input stream from the extremely oversized pieces to prevent damage. The upper and next levels of decks are subjected to blinding (see Figure 1(b)) which causes screen overloading and technological process interruption. Some methods are proposed for automatic cleaning but only for small size meshes. Operators of large-scale screens have to manually clean up the accumulated mass of material and to check the designed trajectory (orbit) of motion (see Figure 1(c)). On the other hand, falling pieces of the material produce force impacts of large amplitude; therefore, those stochastics by nature disturbance should be accounted in diagnostic procedures to prevent false alarms.

The various approaches to screen investigation and applied modifications of their structure and technological regimes tuning are overviewed in [1–3]. The assigned oscillating regimes of screens determine the diagnostics and monitoring methods. Two main classes of screens are known: resonant type and above resonance type. The resonance regime is desirable; however, its control is complicated because of sieving process being vulnerable to changes of bulk material thickness, particles distribution over the layer, and their properties (fractional composition, material humidity, and tendency to fracture) [4–6]. Separation of fine materials subjected to adhesion is achieved by increasing the excitation frequency.

One of the ways to provide better sieving is to excite parametric vibration [7–9] and nonlinear oscillations with a broader frequency range [3, 10]. However, drives with a constant frequency of excitation are the most used case in the industry.

The natural modes of screen and multiply particles motion are efficiently investigated by the methods based on finite and discrete elements [11–19] to ensure minimal structural stresses and required trajectories. However, these methods are very computer resources consuming in research and optimisation. Besides it, a detailed 3D model of the certain screen is required (not always available) as well as design of particles configuration and statistical fractions distribution in the input flow. Therefore, dynamical analysis of vibrating screen as a rigid body filled with a bulk material can be conducted based on the reduced degree-of-freedom spring-mass models [20–23].

Supporting springs are the key elements because their stiffness influences the overall process and the particles' trajectory. Although air-filled or elastomer springs could be advantageous in operation, they may exhibit nonlinear behaviour [24, 25], whereas steel springs have linear stiffness within a working range of deformation. Nevertheless, the side bending displacement of steel springs is nonlinearly related to a vertical stiffness [26, 27] that can result in specific dynamical effects.

Each of the four supporting units on the screen has several helical springs in which geometry (Figure 2(b)) and steel properties are gradually deteriorated. As a consequence, the amplitude of forced vibration and natural frequencies of the screen is changing. To control springs stiffness and the dynamical characteristics of the system, the authors in [28] proposed the use of shape memory alloy in case of the resonant regime of vibrating screen for fine-tuning of natural frequency. Standard springs made of alloy steels are subjected to corrosive wear and cyclic fatigue [29, 30]. The most efficient remedy against failures of springs is the cryogenic treatment of high carbon and alloy steels [31]. Application of nondestructive testing (infrared imaging, magnetic, ultrasound, etc.) is challenging because of the complex geometry of helical springs and nonstop operation mode of a processing plant. Therefore, it is preferable to use the signals of vibration sensors installed on the springs (Figure 2(a)).

Several vendors of condition monitoring systems are known in the market proposing options for vibrating machines. Some of those systems have the specialised functions for diagnostics, namely, of the sieving screens.

(i) CONIQ (Schenck) is a condition monitoring system, which can detect possible defects in the screen based on a six-dimensional vibration measurement using piezoelectric accelerometers and bearings temperature [32].

(ii) FAG SmartCheck (Schaeffler) system monitors vibrations to recognise damage in a filled vibrating screen: settling of screen mats, loose springs, and spring breakage. Monitored parameters are vibrations, the temperature of bearings, speed of rotation, and screen load. Diagnostic methods include time series of vibration, envelope curve, speed, spectrum, and trend analysis [33].

(iii) ScreenWatch (Check) (Metso) system is based on wireless self-powered sensors and detects a

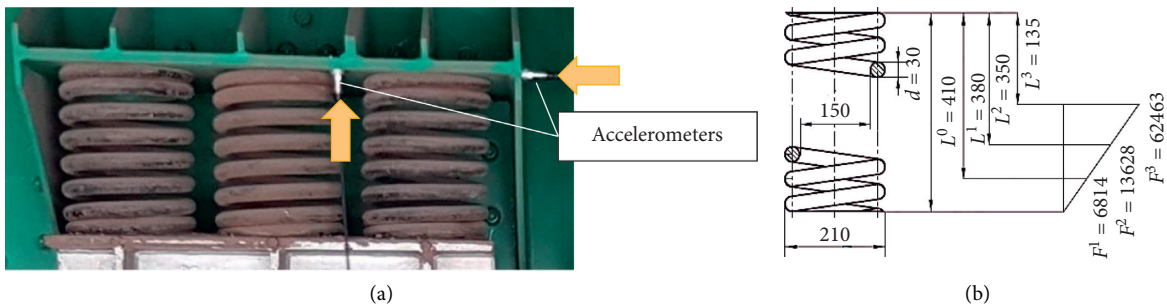

(a) (b)

Figure 2: Supporting unit with three springs and vibration sensors (a); geometry and deformations of a single helical spring (b).

deviation in nominal screen motion caused by broken springs and damaged bearings, incorrect rotational speed, and unbalanced masses settings [34].

(iv) Copperhead (SKF) system monitors vibrating screens faults including gears, bearings, screen body, and decks damage and overloading [35].

All these systems are based on the standard algorithms of vibration monitoring aimed at detection of local defects in the bearings. However, the falling copper ore is a source of the random impulsive noise in vibration signals. Recording the pure signal of load supposes the use of strain sensors installed on the different elements [36] or rotating shafts [37, 38] with appropriate wireless tools. Methods of drivelines diagnostics with special instrumentation [39] are not applicable in case of spring diagnostics. The monitoring of springs technical condition by the electrical drives currents [40, 41] is not feasible because of only slow rotational components reflection in these signals.

One of the specific features in vibrating machines is the continuous displacement of the most loaded zone on the outer race of rolling bearings of the vibrators shafts [42]. Only special series of ball bearings are applicable in these machines. The stiffness of bearings housing should be equivalent in all directions to provide reliable and durable operation. Problems of rotor-roller bearing-housing system (RBHS) interactions based on the dynamic modelling method and including the additional excitation zone are investigated in work [43].

Numerous statistics are known for contact defects detection in vibration signals of rotating machines; most of them are in frequency domain, although time domain can be as well used for defects detection. The authors in [44] compared twenty-five statistical characteristics of time-domain vibration signal and proposed a new spalling detection method accounting spectrum amplitude ratio and statistical features.

The advanced methods are developed for vibration signal processing recorded on a hammer crusher [45–48], which includes stochastic impulsive components [49, 50] having non-Gaussian distribution. Stochastic load analysis in vibrating screens is investigated in [51, 52], but the statistical approach is mainly implemented for analysis of particle distributions [53]. The diagnostics of heavy machines by the multibody nonlinear dynamical models is given in [54–56] with accounting stochastic features of the external impacts [57]. Therefore, kinetic [58] and dynamical [59] models are as well applicable for diagnostic features derivation of vibrating screens encompassing supporting springs [60].

In theory, identification of the stiffness characteristics in multibody systems is conducted by combining experimental frequency response functions (FRF) and "inverse problem" solving. Several schemes were established and tested to determine joining stiffness in a set of elements [61], although only for linear stiffness estimation.

Diagnosis algorithms are constructed in [62] based on the dynamical model. The authors considered modelled vibration signal and six variants of stiffness changes as a spring defect. Assigned changes in stiffness have a small effect in amplitudes, and springs defects are hard to recognise under conditions of heavy-tailed noise. A 3-DOF dynamical model is used in [63] to investigate faults in the vibrating screen. Vibrating screen fault detection and signal processing algorithms are given in [64]. The method of diagnostics for springs of vibrating screen based on stiffness identification is developed in [65]. A method for damping spring failure diagnosis of a large vibrating screen is proposed in [66] based on static deformation test. Influence of material and produced loads on screen vibration is analysed in [67, 68].

A phase space plot (PSP) is a graphical method in analysis of nonlinear systems, which is rarely used in diagnostics [69–72]. PSP is a trajectory in angular or linear coordinates and their derivatives. PSP is more efficient in the vicinity of the bifurcation points when the dynamical system is susceptible to a small change of parameters.

Taking into account the similar dynamic features of all systems with bilinear stiffness characteristics, numerous methods developed for cracks diagnostics in structural health monitoring of stressed bending beams or shafts and gears [73] can be considered in our case for failure diagnostics springs. Diagnosis of bilinear systems is realised by the analysis of natural modes [74]. The estimates of damping and natural frequency are used as the diagnostic parameters in [75].

This paper highlights a model-based approach with other signal processing techniques for the diagnostics of springs stiffness reduction or crack initiation in vibrating screen as the nonlinear system. The proposed model includes alpha-stable

stochastic impulsive components produced by the falling pieces of material. Results of industrial measurements of vibration signals are used for dynamic model verification.

2. Methodology of the Vibrating Screens Diagnostics

The investigated sieving screen (SWR-3 PZ2-2.2-6.0) separates the incoming material into three grades: <40, 40–110, and >110 mm. The maximum dimensions of the ore pieces falling into the sieve are $500 \times 500 \times 300$ mm. The screen supports consist of four sections with 3 springs in each corner with parameters $\varnothing 210/30 \times 410$ mm. Nominal stiffness of a full set of 12 springs and proper tuning of vibrators have to provide a designed orbit or trajectory of screen motion (see Figure 1(c)). The screen is driven by two electric motors and individual belt transmissions with 0.582 ratios of pulleys diameters. Special spherical roller bearings (FAG T41A series) are used on the shafts of unbalanced exciters. The unbalanced masses are placed on the shafts under safety covers and allow changing amplitudes of vibration by choosing the preinstalled different numbers of inserted pads. The default value of producer for screen decks vibration amplitude is 11 mm at a rotation speed of 850 min^{-1} and with 2 pads on the ends of every shaft. Usually, vibrators are self-synchronised either by the kinematic gear couplings or dynamically [76], but the investigated machine is designed without a kinematic coupling between drives. Hence, depending on the oscillations tuning (accuracy of unbalanced masses mounting, a bias of motors speed control), the screening process may be affected and additional stresses may appear in the elements.

The monitoring of sieved material at input and output is realised by the digital cameras. To prevent abrupt failures, a permanent monitoring system (Figure 3) is installed on the investigated vibrating screen of the mining company.

Currently, further research is initiated to scale up the functionality of the existing system and to improve its performance on supporting springs diagnostics and technological process monitoring.

2.1. Dynamical Model. A dynamical model is proposed ,assuming screen as a rigid body vibrating on the four supporting units having bilinear stiffness characteristics in case of cracks initiating. Hence, six degrees-of-freedom (6-DOF) are accounted including three axes (X, Y, and Z) of linear displacements and three angles (γ, φ, and θ) of rotation correspondingly. Calculation scheme for the analysis of vibrating screen is shown in Figure 4(a).

Periodical excitation from two unbalanced vibrators (see Figure 5(a)) is considered as a deterministic part of external forces:

$$F_U(t) = m\varepsilon\omega^2 \sin(\omega t + \Delta\psi), \tag{1}$$

where m are the masses of each unbalanced vibrator; ε is the eccentricity; ω is the speed of shaft rotation (rad s^{-1}); and $\Delta\psi$ is the phase difference between two rotating vibrators because of detuning.

Stochastic part of the equivalent external force $F_{\Sigma Y}(t)$ applied to the screen consists of two components (see Figure 5(b)):

(1) The first component $F_{\Sigma Y1}(t)$ having alpha-stable distribution $S(\alpha; \beta; \sigma; \mu)$ includes impacts from the input flow. Median point of equivalent force application (p.f.a.) has relative displacements $L_X(t)$ and $L_Z(t)$ from a nominal position with Gauss distribution $N(\mu; \sigma)$. Some technological parameters, namely, feed specific volume, fractions sizes, and conveyor geometry, affect the external force distribution.

(2) The second component $F_{\Sigma Y2}(t)$ includes impacts which happen during periodical motions of particles over the decks. The input $+ M_{\text{in}}(t)$ and output $- M_{\text{out}}(t)$ flow (see Figure 4(b)) should satisfy mass balance condition, which assumes that the dynamical system has a constant mass during oscillations.

The subsequent sections of the screen may have different inclination angles [77]. Therefore, spring-mass model verification based on vibrations measurement has to be based on trigonometric relations between the centre of mass coordinates in the model and sensors positions on the screen.

Parameters of impulsive force alpha-stable distribution $S(\alpha; \beta; \sigma; \mu)$ depends on material fraction, the linear speed of transportation conveyor and its specific loading, and distance from the end of conveyor to the upper deck of screen. Simulation of stochastic components in the dynamic model is based on formulas proposed in [78, 79].

For $\alpha \neq 1$,

$$\begin{aligned} X &= S_{\alpha,\beta} \times \frac{\sin\left(\alpha\left(V + B_{\alpha,\beta}\right)\right)}{(\cos V)^{1/\alpha}} \times \left(\frac{\cos\left(V - \alpha\left(V + B_{\alpha,\beta}\right)\right)}{W}\right)^{(1-\alpha)/\alpha} + \mu, \\ S_{\alpha,\beta} &= \sigma \times \left[1 + \left(\beta \tan\frac{\pi\alpha}{2}\right)^2\right]^{1/2\alpha}, \\ B_{\alpha,\beta} &= \frac{\arctan(\beta \tan(\pi\alpha/2))}{\alpha}, \end{aligned} \tag{2}$$

and for $\alpha = 1$,

$$\begin{aligned} X = {} & \sigma \times \frac{2}{\pi}\left[\left(\frac{\pi}{2} + \beta V\right)\tan V - \beta \log\left(\frac{(\pi/2) W \cos V}{(\pi/2) + \beta V}\right)\right] \\ & + \frac{2}{\pi}\beta\sigma \log\sigma + \mu, \end{aligned} \tag{3}$$

where $V(x) = \pi\ U{-}\pi/2$ is the uniform distribution $U(-\pi/2, \pi/2)$; $W(x) = \lambda \exp(-\lambda x)$ is the exponential distribution with the mean $1/\lambda = 1$; $\alpha \in [0, 2]$ is the stability parameter; $\beta \in [-1, 1]$ is the skewness; $\sigma > 0$ is the scale factor; and $\mu \in R$ is the mean location.

Finally, the system of the differential equations governing the dynamical model is as follows:

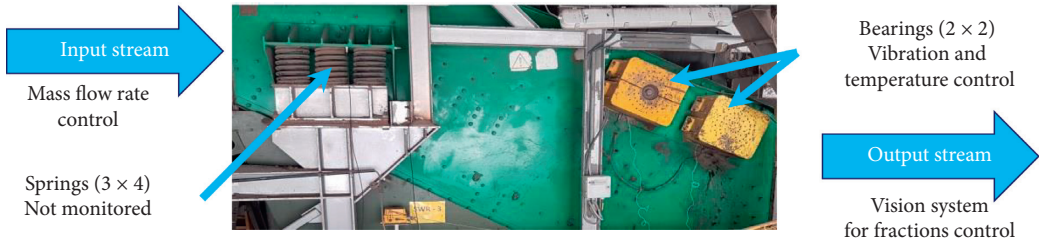

Figure 3: Components of the monitoring system on the vibrating screen (nondriven side) with two exciters.

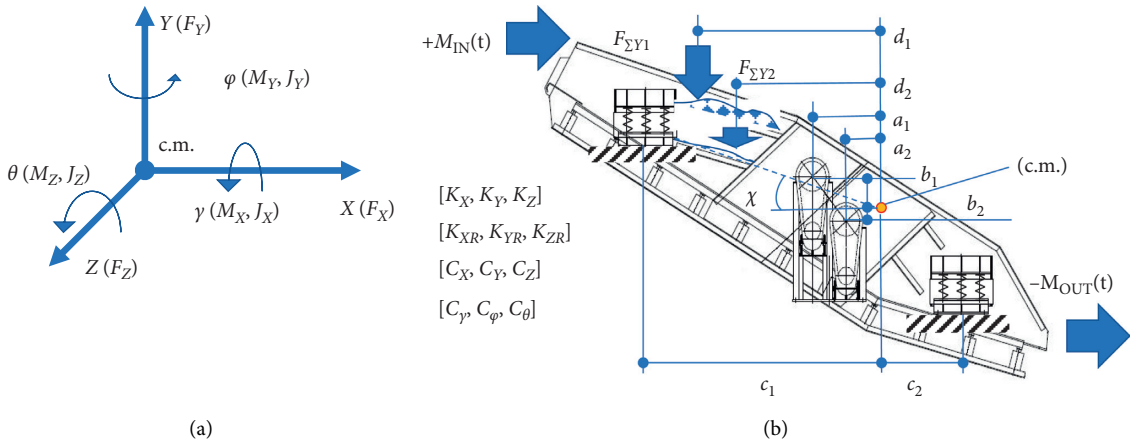

Figure 4: The dynamical model of the vibrating screen: 6-DOF system of coordinates (a); geometrical parameters (b).

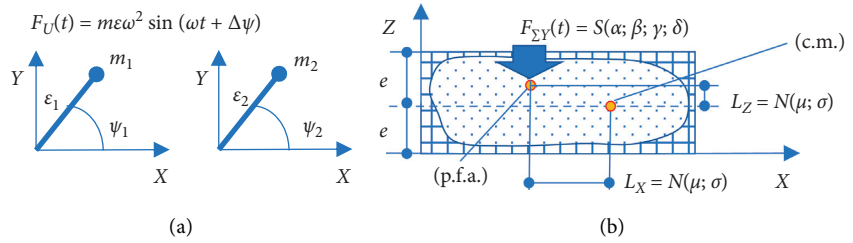

Figure 5: Components of external forces applied to the screen: deterministic (a) and stochastic (b).

$$\begin{cases} M\ddot{x} + \dot{x}C_x + xK_x = A\,F_U(t) - k_1 F_{\Sigma Y}(t)\cos(\chi), \\ M\ddot{y} + \dot{y}C_y + yK_y = B\,F_U(t) - F_{\Sigma Y}(t), \\ M\ddot{z} + \dot{z}\,C_z + z\,K_z = C\,F_{\Sigma Z}(t), \\ J_X\ddot{\gamma} + \dot{\gamma}C_\gamma + \gamma K_{XR} = F_{\Sigma Y}(t)L_X(t), \\ J_y\ddot{\varphi} + \dot{\varphi}C_\varphi + \varphi K_{YR} = F_{\Sigma Y}(t)\cos(\chi)L_Z(t), \\ J_z\ddot{\theta} + \dot{\theta}C_\theta + \theta K_{ZR} = D\,F_U(t) + F_{\Sigma Y}(t)L_Z(t), \end{cases} \tag{4}$$

where $K_X = (K_{X1} + K_{X2} + K_{X3} + K_{X4})$ is the stiffness of springs in horizontal directions x and z ($K_Z = K_X$); $K_Y = (K_{Y1} + K_{Y2} + K_{Y3} + K_{Y4})$ is the stiffness of springs in vertical direction y; K_{XR}, K_{YR}, and K_{ZR} are the torsional stiffness of angular motion; C_X, C_Y, and C_Z are the damping of vibrations; C_γ, C_φ, and C_θ are the damping of rotations; k_1 is the coefficient of contact interaction; χ is the screen inclination angle; $F_{\Sigma X}(t)$, $F_{\Sigma Y}(t)$, and $F_{\Sigma Z}(t)$ are the stable distribution $S(\alpha; \beta; \gamma; \delta)$ of stochastic equivalent force from material impacts; L_X and L_Z are normally distributed $N(\mu; \sigma)$ in a position of equivalent force $F_{\Sigma Y}(t)$ application, where μ is the mean value; σ is the standard deviation from nominal position (middle of the deck); A, B, C, and D are the functions of χ and θ angles and $\psi_{1,2}$ angles of two vibrators rotation; a_i, b_i, c_i, and d_i are the position of the centre of mass (c.m. and p.f.a).

The system of differential equations was integrated by the Runge–Kutta method of 4th order with fixed step in time. The external stochastic impacts are generated in advance as a vector of numbers and are introduced into the right part of corresponding equations at every time step.

2.2. Simulation of Springs Wear. The predictive maintenance of vibrating screens requires detection of two main failure modes of springs: reduced stiffness and cracks. The usual approach of machine disassembling and visual inspection, e.g., retained deformation of every spring, is not possible.

After defect initiation and growing in any spring, its linear stress-strain characteristic transforms into the bilinear function; i.e., compression and stretching stiffness are different. The lateral spring stiffness depends on where the defect is situated. Within the vertical plane of vibrators rotations, vibration signal may have signs of springs damage; otherwise, these defects are undetectable.

In order to construct the diagnostics rules, the dynamical model is simulated, and the parameters are shown in Table 1.

The elastic forces of supporting springs with bilinear stiffness are shown in Figure 6(a). The simulated stochastic force impacts from the input flow of material pieces in the time domain are represented in Figure 6(b), and its significantly skewed distribution is in Figure 6(c).

Time series of vibration and spectrums for healthy and cracked springs are given in Figure 7. Under the action of external impact, the dynamical system of vibrating screen responds by transient vibration in the different coordinates of motion. The transient process is quickly attenuated (Figure 7(a)). In theory, the shift of resonant frequency from its nominal value corresponding to a new spring may be a diagnostic parameter. However, maintenance staff replaces springs not simultaneously in every supporting unit, which has 3 or more springs on other types of screen. Therefore, a single spring stiffness variation is difficult to discriminate, especially due to its typically very small values (Figure 7(b)). Nonlinear stiffness of springs results in harmonics of the main natural vibration mode (1–2 Hz) and modulation side-band at the excitation frequency (15 Hz) as is shown in Figure 7(c).

The orbit of screen motion reconstructed from the orthogonal vibration signals and phase space plots in coordinates of vertical displacement and velocity are shown in Figure 8. The orbit and phase space plots are changing with spring stiffness reduction and crack appearing.

Dynamical model simulations are represented in Figure 9 with different parameters of machine body vibration concerning the springs bilinear stiffness change (decrease) from 100% to 50% of the upper positive branch of deformation characteristic in Figure 6(a). Step of change is 1% for 90–100% range and 10% for the 90–50% range.

Graphs show that almost all parameters have a linear relation with vertical (Y-axis) stiffness change. Horizontal amplitude (dx) in Figure 9(a) has a specific hill above 90% and then goes linearly while vertical amplitude (dy) is always linear. The sensitivity of these parameters is very small ~0.03 mm/50%. Orbit slope (x; y) in Figure 9(b) is exactly linear but has weak sensitivity to stiffness change ~0,05°/50%. The form factor of the phase space plot (dVy/dy) in Figure 9(c) is almost linear within the whole range of stiffness change while the amplitude of vibration velocity dVy is always linear. Sensitivity of velocity is 0.03 (mm/s)/50%.

Natural frequency (x1 Yfreq) and amplitudes of its first (x1 Yamp) and second (x2 Yamp) harmonics in the Figure 9(d) shows linear behaviour but with opposite relation: frequency and first harmonic go down while second harmonic amplitude increases. The sensitivity of natural frequency is 0.4 Hz/50% and the reaction of its harmonics amplitudes is ~0.2. . .1.0 mm^2/50%.

Table 1: The parameters taken in simulations of the dynamical model.

	Parameter	Notation	Value	Units
1	Vibrator 1 horizontal position	a_1	1.400	m
2	Vibrator 2 horizontal position	a_2	0.800	m
3	Vibrator 1 vertical position	b_1	0.900	m
4	Vibrator 2 vertical position	b_2	0.300	m
5	Position of upper springs	c_1	2.600	m
6	Position of lower springs	c_2	1.300	m
7	Point of force $F_{\Sigma Y1}$ application	d_1	2.200	m
8	Point of force $F_{\Sigma Y2}$ application	d_2	1.200	m
9	Width between the springs	$2e$	2.200	m
10	Mass of empty screen	M	15 230	kg
11	Inertial moment	J_X	2.08×10^5	kg·m^2
12	Inertial moment	J_Y	4.25×10^5	kg·m^2
13	Inertial moment	J_Z	6.13×10^5	kg·m^2
14	Stiffness of linear motion	K_X	2.12×10^6	N/m
15	Stiffness of linear motion	K_Y	4.80×10^6	N/m
16	Stiffness of linear motion	K_Z	2.12×10^6	N/m
17	Stiffness of rotation	K_{XR}	3.25×10^6	N m/rad
18	Stiffness of rotation	K_{YR}	2.60×10^6	N m/rad
19	Stiffness of rotation	K_{ZR}	5.35×10^6	N m/rad
20	Position of p.f.a.	L_X	0.200	m
21	Position of p.f.a.	L_Z	1.600	m
22	Angle of inclination	χ	22.5	Grad
23	Unbalanced mass of vibrators	m	90	kg
24	Speed of vibrators rotation	ω	88	rad/s
25	Eccentricity of vibrators	ε	0.210	m
26	The phase difference of vibrators	ψ	5	Grad
27	Damping of linear motion	C_X, C_Y, C_Z	1.97	s^{-1}
28	Damping of rotation	C_γ, C_φ, C_θ	4.29	rad s^{-1}
29	S distribution, exponent	α	1.2	—
30	S distribution, skewing	β	1	—
31	S distribution, scaling	γ	0.5	—
32	S distribution, localisation	δ	1000	N
33	N distribution, mean value	μ	0	m
34	N distribution, standard deviation	σ	0.1	m
35	Input-output flows of material	M_{in} , M_{out}	236	kg/s

3. Industrial Measurements

Vibration measurements are accomplished by the Kistler LabAmp 5165A 4-channel modules and accelerometers K-Shear 8702B500. The other instrumentation included National Instruments 9233 4-channel modules and accelerometers EC Systems VIS-311A and Endevco 751–10. All

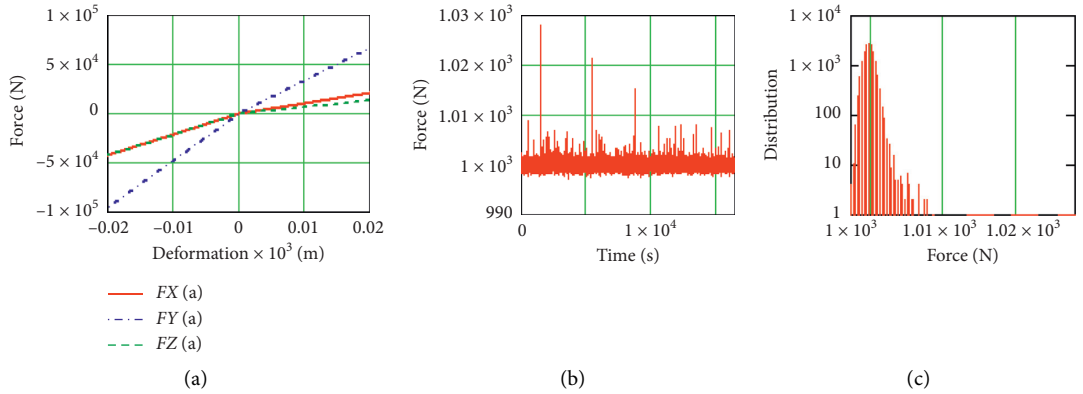

Figure 6: Bilinear stiffness of springs (a); stochastic force in the time domain (b); and force distribution (c).

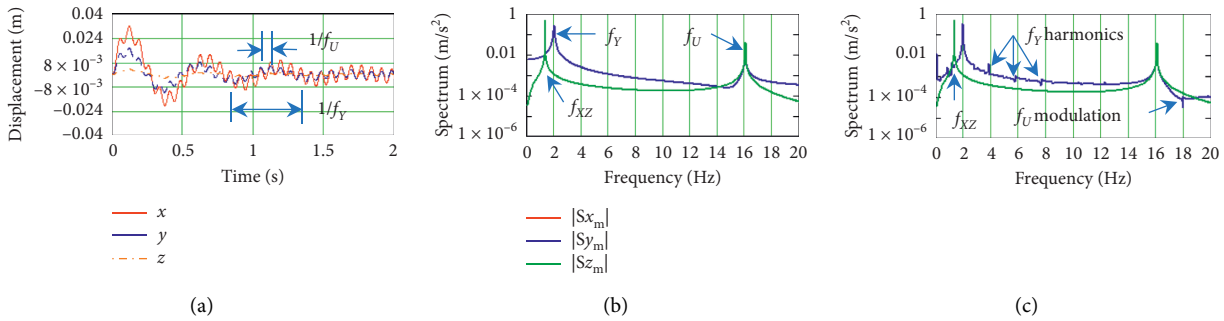

Figure 7: Transient vibration (a); vibration spectrums for new (b); and cracked (c) spring.

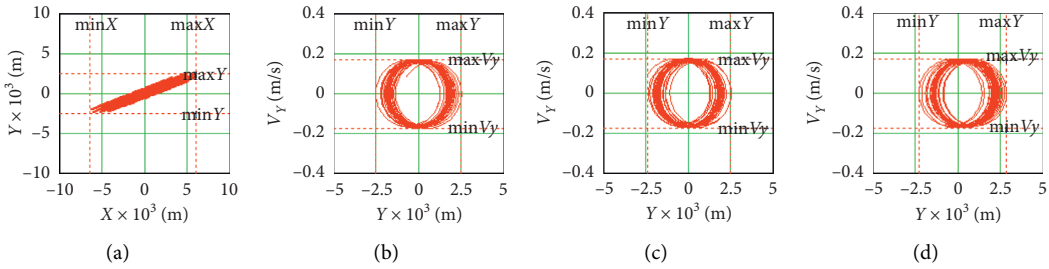

Figure 8: Motion orbit (a) and PSP of vibrating screen: (b) with new springs; (c) with less by 20% stiffness K_Y; (d) with a crack in spring (nonlinear K_Y).

sensors have an extended range of measurement (±50–500 g) and sensitivity (10–100 mV/g). Positions of accelerometers and measurement directions are shown in Figure 10.

3.1. Screen Motion Orbits. The spatial motion stipulated by the screen designers (see Figure 1(c)) is estimated by the vertical and horizontal vibration signals measured on every supporting unit (Figure 11). Notations of signals correspond to the following: S, springs; *B*, bearings; *L* and *R*, left and right side; *U* and *D*, upper and down; *H* and *V*, the horizontal and vertical direction of measurement.

The time series on springs contain the main dominating frequency of excitation about 15 Hz, which corresponds to vibrators shafts rotations. As the vibration recordings from the left and right sides are not synchronised, the instant phase relations have a sense only for every side separately.

The trajectories (orbits) obtained by the double integration of the original acceleration signals and phase space plots are represented in Figure 12. The numerical diagnostic parameters determined by the measured vibration are shown in Table 2. Orbits on the left springs are inclined to the horizon by 66–67° and by 47–51° for the right side. Amplitudes of vertical vibrations are about ±5 mm and those of horizontal ones are about ±3–4 mm and lay within the design values range (values of projections on *X* and *Y* axis in Figure 1(c)). The phase space plots are quite different for the left and right sides even for the similar orbit graphs that give a piece of additional diagnostic information for further analysis.

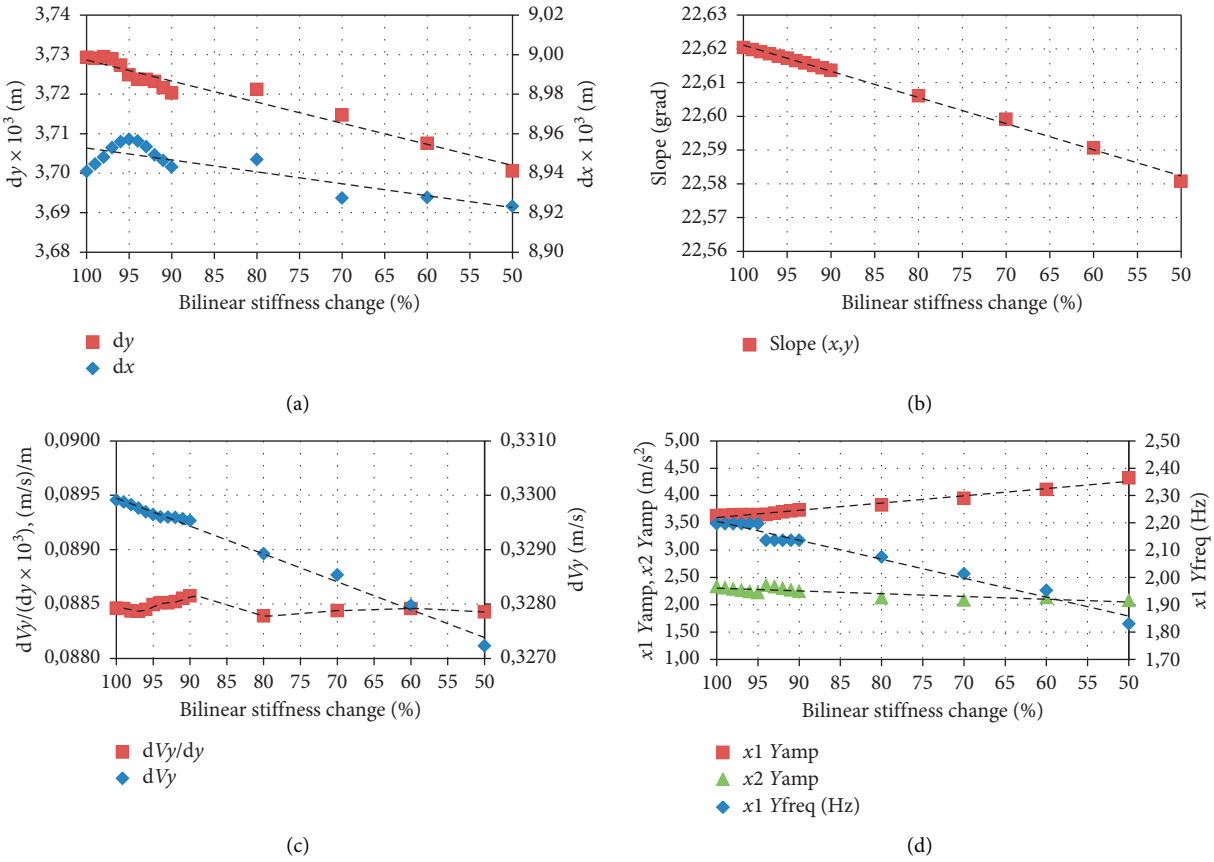

FIGURE 9: Investigation on the model diagnostic parameters of vibrating screen springs: (a) orbit size (dx; dy); (b) orbit slope (x; y); (c) form of phase space plot (dYy/dy) (dVy); (d) natural frequency (x1 Yfreq) and amplitudes of first (x1 Yamp) and second (x2 Yamp) harmonics.

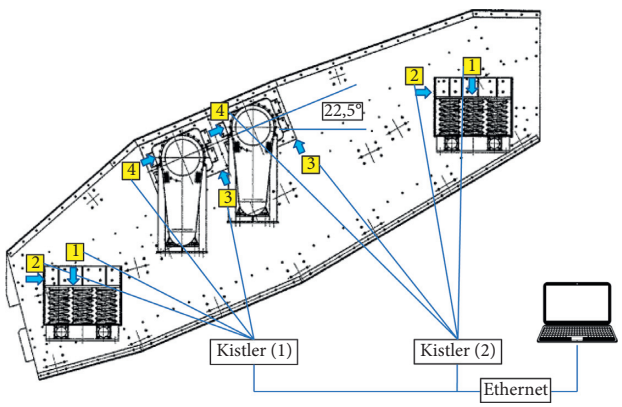

FIGURE 10: Places and directions of accelerometers mounting on the vibrating screen.

The configuration of orbit greatly depends on the nonlinear trends in the initial signal of acceleration, which affects the final view of the displacement signal after double integration operations. This problem is resolved by the proper selection of a time slot for signal analysis without the remarkable transients from falling pieces of material. Also, the polynomial trend of 8th order is removed from the initial signals at every stage of their integration.

3.2. Verification of Damping Factors and Resonant Frequencies. The resonant frequencies and damping in the system are identified by the analysis of the transient response from the falling pieces of material (see Figure 13). The verified values of damping factors are given in Table 1. Because frequency-independent damping is admitted in the model, some discrepancy may appear in exponential decay values determined experimentally. In the future, it is desirable to synchronise the vibration and video records for joint processing to obtain qualitative estimations of stochastic impacts from the input flow of material. The frequencies of identified natural modes of the investigated screen are represented in Table 3 and low-frequency spectrums are shown in Figure 14.

Because of response deviation in the used types of accelerometers in the low-frequency range (1–2 Hz), natural frequencies identification and separation need another type of sensors. For comparison, the result of the bump test conducted by Metso Company with the ScreenCheck system on a similar type of vibrating screen is shown in Figure 15.

Three peaks in Figure 15 within the frequency range of 60–180 rpm (1–3 Hz) are the lowest modes of this screen and quite similar to values in the investigated screen (see Table 3). Other peaks in Figure 15 correspond to higher modes and vibrators excitation (dotted line is a maximal speed of exciters rotation).

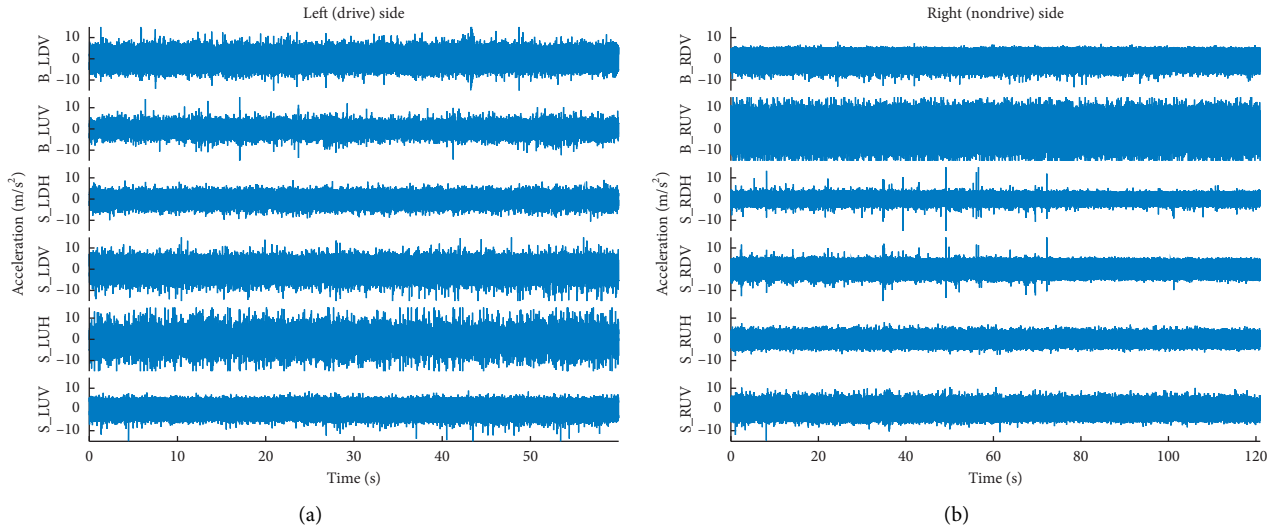

Figure 11: Signals of screen acceleration measured on the left (drive) side (a) and right (nondrive) side (b).

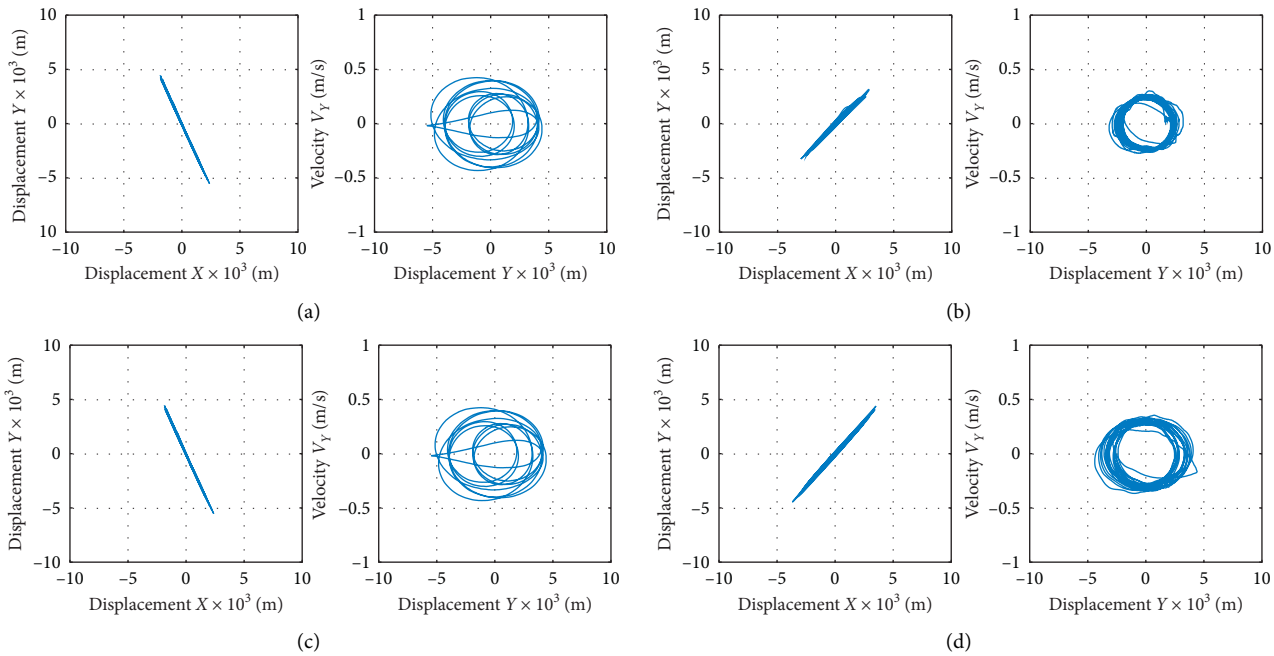

Figure 12: Vibration orbits and phase space plots on springs: upper left (a) and right (b); down left (c); and right (d).

Table 2: The diagnostic parameters of measured vibration.

Pos.	$dy \times 10^3$ (m)	$dx \times 10^3$ (m)	Slope (grad)	dVy (m/s)	$dVy/(dy \times 10^3)$ (m/s) (m)	×1 Yamp (m/s²)	×2 Yamp (m/s²)	×1 Yfreq (Hz)
LU	9.92	4.22	66.9	0.86	0.086	3.50	0.66	1.7
LD	9.88	4.18	67.1	0.85	0.087	4.10	0.66	1.7
RU	6.40	5.87	47.5	0.58	0.090	3.16	0.41	1.8
RD	8.83	7.18	50.9	0.72	0.082	3.36	0.75	1.7

4. Discussion

The screen body is supported by a set of springs. If change of spring stiffness appears (for example, due to wear or crack), vibration of the screen will be asymmetrical. It may lead to damage of sieving screen elements.

Each suspension unit of the screen consists of 2–4 springs. In such a case, detection of single failed spring by the

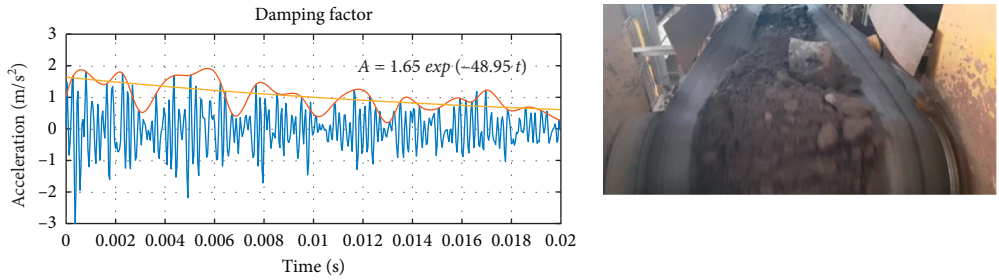

Figure 13: Transient vibration on the spring (a) and image of the input piece of material (b).

Table 3: The natural frequencies of the vibrating screen.

	Linear motion frequencies			Rotation motion frequencies		
	f_X	f_Y	f_Z	f_γ	f_φ	f_θ
Hz	1.8	2.6	1.8	3.8	2.9	4.1
rpm	108	156	108	228	174	246

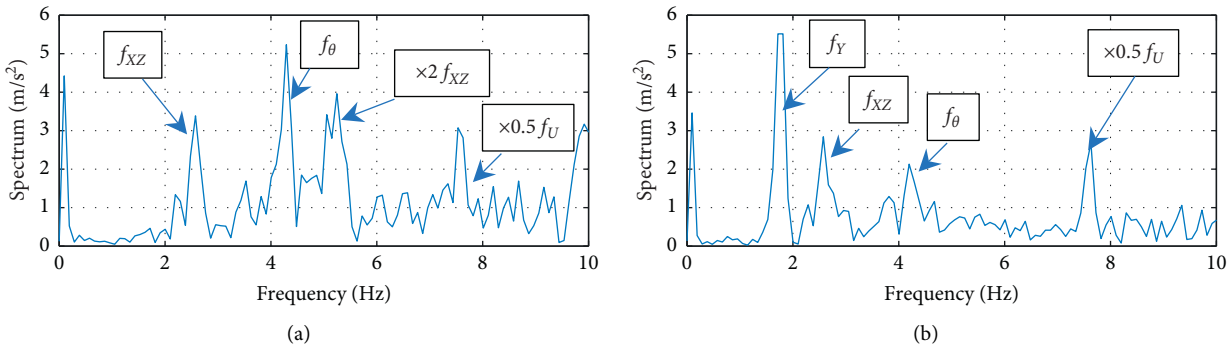

Figure 14: Spectrums of low-frequency vibration on the right side of the upper (a) and down (b) springs.

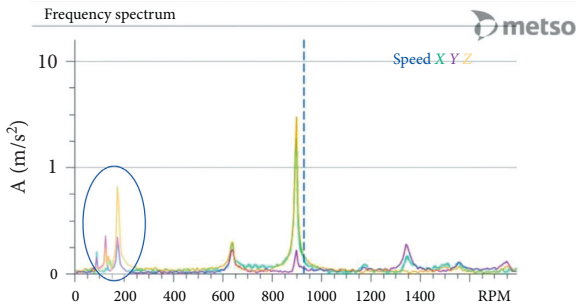

Figure 15: Natural frequencies identified by the bump test in ScreenCheck system (Metso).

static deformation test under load is not possible. It could be concluded by disassembling and visual inspection of suspension unit. The nondestructive testing techniques cannot be used here due to complex geometrical configuration.

The fundamental frequency of screen oscillation caused by unbalanced force (≈15 Hz) significantly exceeds the lowest natural frequency (<3 Hz).

Thus, diagnostics of springs by the resonant frequencies shift and harmonics analysis is quite possible although at least 10 s sampling time is required to provide 0.1 Hz spectrum resolution. That is possible under nonstationary stochastic loads which do not greatly affect natural frequencies. Instead, material impacts excite these frequencies and increase the signal-to-noise ratio at the natural

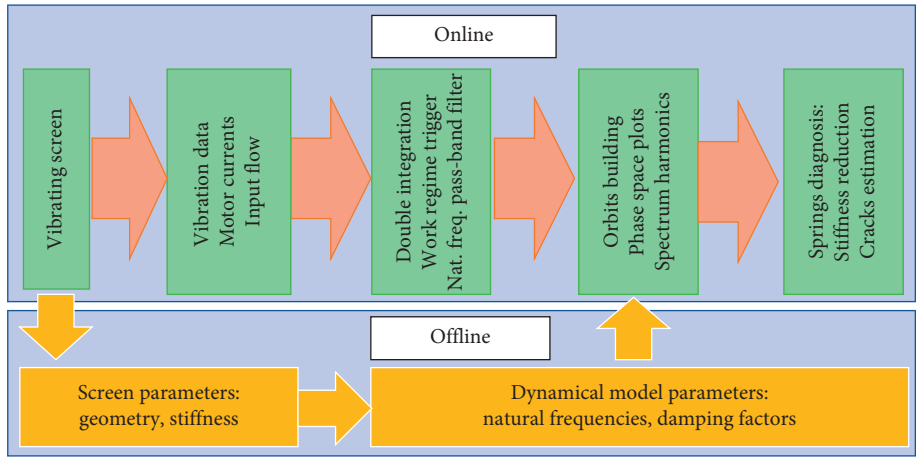

Figure 16: The block diagram of diagnostics procedure implementation.

frequencies range. Besides it, damping factors can be assessed by these impacts as the diagnostic parameters.

The 50% of stiffness reduction (0.5 K_Y) will result in 0.4–0.6 Hz or 25–30% of frequency change from the nominal values about 2 Hz. Taking into account the low natural frequencies 1–3 Hz, this method of diagnostics needs low-frequency displacement measuring sensors.

An advantage of the proposed dynamical model is in accounting the random disturbances occurring from the pieces of sieved ore, which modify amplitude of signal and point of the equivalent force application. The real levels of impacts from the falling pieces of material are much fewer than the amplitude from vibrators and quickly attenuated. Anyway, these impacts excite rotational components in the screen motion which can be as well used as diagnostic parameters.

A localisation of damaged spring among four supporting units might be determined by comparison of 4 signals from different bearings, or sensors installed directly on the supporting units to obtain the more significant difference in displacements between them. The overall block diagram of developed diagnostics procedure implementation is shown in Figure 16. Online and offline steps are divided into separate data flows.

Modification of stiffness of springs and considering nonlinear properties due to crack are noticeable in results of simulations as the harmonics of natural frequencies and side-band modulation of the main forced vibration. Simulation experiments on dynamical model undermined linear relations of orbit size parameters and natural frequency with its first and second harmonics amplitudes. However, the sensitivity of these parameters to bilinear stiffness change is not strong enough.

The proposed parameters of vibrating screen springs monitoring and diagnostics based on natural frequency, its harmonics, and form factor of phase space plot can be generalised for any of three linear coordinates of motion (x, y, z) and angles of rotational vibration (γ, φ, θ). This approach exhibits significant advantages as compared to the spectral methods because it does not require high sampling frequencies.

Using generalised coordinates of screen motion (x, y, z) and derivatives (dx/dt, dy/dt, and dz/dt) enables comprehensive visualisation of the whole portrait of the dynamical system. In this paper, the authors do not address bifurcations of nonlinear system, which make the PSP technique strictly susceptible to minor changes of parameters associated with fault development. Application of the PSP technique in daily practise needs developing qualitative measures of trajectories analysis. This is a plan for future research.

5. Conclusions

In this paper, the dynamical model is applied for the analysis of vibration signals measured on industrial vibrating screens for diagnostics of springs. Introducing into the model the external force from the falling pieces of material with the alpha-stable distribution allows us more correctly to describe real sieving process for the diagnostic purposes. The proposed methods of the vibrating screens monitoring and diagnostics allow detecting theoretically even weak (<10%) deterioration of supporting springs stiffness by the different proposed parameters: motion trajectories (orbits parameters), phase space plots, natural frequencies, and their harmonics. These parameters are related to stiffness decrease and nonlinearity of the dynamical system. Linear model response denotes a good condition of springs without damage. The early detection of spring's stiffness change helps in maintenance to ensure the proper operation of machine. The further efforts will be focused on the study of reliable qualitative measures for measurement data analysis which are immune to non-Gaussian noise. Besides the axial screen vibrations, three rotational low-frequency components can be analysed for discrimination of defects in the different supporting units in case of synchronous measurements on both sides of screen. The changes in frequency response functions at the higher natural modes situated out of vibrators excitation frequency range can be associated with the structural elements failures or loose bolted connections. The damping factor of screen natural vibrations and a phase shift between excitation (measured on the bearings of vibrators) and screen body vibrations at the support units can be assessed as the potential diagnostic parameters. It is

considered installation of 3-axis sensors on every supporting unit.

Data Availability

The data cannot be shared due to non-disclosure agreement with the industrial partner.

Conflicts of Interest

The authors declare that there are no conflicts of interest regarding the publication of this paper.

Acknowledgments

This activity has received funding from the European Institute of Innovation and Technology (EIT), a body of the European Union, under the Horizon 2020, the EU Framework Programme for Research and Innovation. This work was supported by EIT RawMaterials GmbH under Framework Partnership Agreements no. 18253 (OPMO: operation monitoring of mineral crushing machinery). The authors are grateful to the plant maintenance and automation departments staff for the assistance in conducting experimental research on industrial vibrating screen.

References

[1] B. Wen, "Recent development of vibration utilization engineering," *Frontiers of Mechanical Engineering in China*, vol. 3, no. 1, pp. 1–9, 2008.

[2] L. Peng, H. Jiang, X. Chen et al., "A review on the advanced design techniques and methods of vibrating screen for coal preparation," *Powder Technology*, vol. 347, pp. 136–147, 2019.

[3] V. I. Lyashenko, V. Z. Dyatchin, and V. P. Franchuk, "Improvement of vibrating feeders-screens for mining and metallurgical industry," *Izvestiya Visshikh Uchebnykh Zavedenii. Chernaya Metallurgiya = Izvestiya. Ferrous Metallurgy*, vol. 61, no. 6, pp. 470–477, 2018, in Russian.

[4] N. Standish, A. K. Bharadwaj, and G. Hariri-Akbari, "A study of the effect of operating variables on the efficiency of a vibrating screen," *Powder Technology*, vol. 48, no. 2, pp. 161–172, 1986.

[5] H. Dong, C. Liu, Y. Zhao, and L. Zhao, "Influence of vibration mode on the screening process," *International Journal of Mining Science and Technology*, vol. 23, no. 1, pp. 95–98, 2013.

[6] B. Zhang, J. Gong, W. Yuan, J. Fu, and Y. Huang, "Intelligent prediction of sieving efficiency in vibrating screens," *Shock and Vibration*, vol. 2016, Article ID 9175417, 7 pages, 2016.

[7] L. Bak, S. Noga, and F. Stachowicz, "The experimental investigation of the screen operation in the parametric resonance conditions," *Acta Mechanica et Automatica*, vol. 9, no. 4, pp. 191–194, 2015.

[8] L. I. Slepyan and V. I. Slepyan, "Coupled mode parametric resonance in a vibrating screen model," *Mechanical Systems and Signal Processing*, vol. 43, no. 1-2, pp. 295–304, 2014.

[9] S. A. Zahedi and V. Babitsky, "Modeling of autoresonant control of a parametrically excited screen machine," *Journal of Sound and Vibration*, vol. 380, pp. 78–89, 2016.

[10] I. V. Kuzio, O. V. Lanets, and V. M. Gursky, "Substantiation of technological efficiency of two-frequency resonant vibration machines with pulse electromagnetic disturbance," *Naukovyi Visnyk Natsionalnoho Hirnychoho Universytetu*, vol. 3, pp. 71–77, 2013, in Ukrainian.

[11] M. Doudkin, A. Kim, M. Mlynczak et al., "Development and parameter justification of vibroscreen feed elements.," in *Mining Machines and Earth-Moving Equipment*, M. Sokolski, Ed., pp. 82–96, Springer, Cham, Switzerland, 2020.

[12] M. L. Chandravanshi and A. K. Mukhopadhyay, "Analysis of variations in vibration behavior of vibratory feeder due to change in stiffness of helical springs using FEM and EMA methods," *Journal of the Brazilian Society of Mechanical Sciences and Engineering*, vol. 39, no. 9, pp. 3343–3362, 2017.

[13] S. Baragetti and F. Villa, "A dynamic optimization theoretical method for heavy loaded vibrating screens," *Nonlinear Dynamics*, vol. 78, no. 1, pp. 609–627, 2014.

[14] J. Xiao and X. Tong, "Particle stratification and penetration of a linear vibrating screen by the discrete element method," *International Journal of Mining Science and Technology*, vol. 22, no. 3, pp. 357–362, 2012.

[15] A. A. Harzanagh, E. C. Orhan, and S. L. Ergun, "Discrete element modelling of vibrating screens," *Minerals Engineering*, vol. 121, pp. 107–121, 2018.

[16] X. Wu, Z. Li, H. Xia, and X. Tong, "Vibration parameter optimization of a linear vibrating banana screen using DEM 3D simulation," *Journal of Engineering and Technological Sciences*, vol. 50, no. 3, pp. 346–363, 2018.

[17] Z. F. Li, K. Y. Li, X. L. Ge, and X. Tong, "Performance optimization of banana vibrating screens based on PSOSVR under DEM simulations," *Journal of Vibroengineering*, vol. 21, pp. 28–39, 2019.

[18] Z. Q. Wang, L. P. Peng, C. L. Zhang et al., "Research on impact characteristics of screening coals on vibrating screen based on discrete-finite element method," *Energy Sources, Part A: Recovery, Utilization, and Environmental Effects*, vol. 42, no. 16, 2019.

[19] F. Safranyik, B. M. Csizmadia, A. Hegedus, and I. Keppler, "Optimal oscillation parameters of vibrating screens," *Journal of Mechanical Science and Technology*, vol. 33, no. 5, pp. 2011–2017, 2019.

[20] B. C. Song, C. S. Liu, L. P. Peng, and J. Li, "Dynamic analysis of new kind elastic screen surface with multi degree of freedom and experimental validation," *Journal of Central South University*, vol. 22, no. 4, pp. 1334–1341, 2015.

[21] Z. Zhang, Y. Wang, and Z. Fan, "Similarity analysis between scale model and prototype of large vibrating screen," *Shock and Vibration*, vol. 2015, Article ID 247193, 7 pages, 2015.

[22] X. Yang, J. Wu, H. Jiang et al., "Dynamic modeling and parameters optimization of large vibrating screen with full degree of freedom," *Shock and Vibration*, vol. 2019, Article ID 1915708, 12 pages, 2019.

[23] P. Krot and R. Zimroz, "Methods of springs failures diagnostics in ore processing vibrating screens," *IOP Conference Series: Earth and Environmental Science*, vol. 362, Article ID 012147, 9 pages, 2019.

[24] S. Gong, S. Oberst, and X. Wang, "An experimentally validated rubber shear spring model for vibrating flip-flow screens," *Mechanical Systems and Signal Processing*, vol. 139, Article ID 106619, 2020.

[25] A. F. Bulat, V. I. Dyrda, M. I. Lysytsya, and S. M. Grebenyuk, "Numerical simulation of the stress-strain state of thin-layer rubber-metal vibration absorber elements under nonlinear deformation," *Strength of Materials*, vol. 50, no. 3, pp. 387–395, 2018.

[26] G. Ene and N. Sporea, "Approaches regarding the calculus of the elastic system of the initial vibrating screens," *Revista de Chimie (Bucharest)*, vol. 67, no. 2, pp. 308–313, 2016.

[27] G. Ene, "Design of the elastic system of the vibrating screens," *Revista de Chimie (Bucharest)*, vol. 60, no. 11, pp. 1123–1128, 2009.

[28] W. Raczka, M. Sibielak, J. Kowal, and J. Konieczny, "Application of an SMA spring for vibration screen control," *Journal of Low Frequency Noise, Vibration and Active Control*, vol. 32, no. 1-2, pp. 117–132, 2013.

[29] L. D. Vizcaya, C. Gonzalez, G. Mesmacque, and T. Hernandez, "Multiaxial fatigue and failure analysis of helical compression springs," *Engineering Fatigue Analysis*, vol. 13, no. 8, pp. 1303–1313, 2006.

[30] V. Gursky and I. Kuzio, "Strength and durability analysis of a flat spring at vibro-impact loadings," *Eastern-European Journal of Enterprise Technologies*, vol. 5, no. 7, pp. 4–10, 2016.

[31] P. Krot, S. Bobyr, and M. Dedik, "Simulation of backup rolls quenching with experimental study of deep cryogenic treatment," *International Journal of Microstructure and Materials Properties*, vol. 12, no. 3-4, pp. 259–275, 2017.

[32] Schenk, *CONiQ Online. Condition Monitoring for Screening Machines and Vibrating Feeders*, 2019, https://www.schenckprocess.com/products/coniq-condition-monitoring.

[33] Schaeffler, *FAG SmartCheck. Machinery monitoring for every machine*, 2012, https://www.schaeffler.com/remotemedien/media/_shared_media/08_media_library/01_publications/schaeffler_2/tpi/downloads_8/tpi_214_en_us.pdf.

[34] Metso, *ScreenWatch. Screen Condition Monitoring. Enhancing Screen Availability*, 2019, https://www.metso.com/globalassets/saleshub/documents---episerver/screenwatch_screen_monitoring_2014_lr.pdf.

[35] SKF, *Fault Detection for Mining and Mineral Processing Equipment*, 2001, http://evolution.skf.com/fault-detection-for-mining-and-mineral-processing-equipment-2/.

[36] R. Onofrei, G. Dobre, R. F. Mirică, and M. Pali, "On measurement and processing data of the real loading: application to cement equipment components," in *Power Transmissions, Mechanisms and Machine Science*, G. Dobre, Ed., vol. 13, pp. 701–713, Springer, Dordrecht, Netherlands, 2013.

[37] P. V. Krot, A. Y. Putnoki, O. M. Klevtsov, and A. A. Ermolenko, "Experimental studies and industrial testing of methods for reducing dynamic loads in the gearbox drivelines of roughing stands of NTLS 1680," in *Proceedings of the 5th Congress of Rolling*, pp. 523–529in Russian, Cherepovets, Russia, October 2003.

[38] P. V. Krot, "Telemetering systems for monitoring dynamic loads in drive lines of rolling mills," *Vibration of machines: measurement, reduction, protection*, vol. 1, pp. 31–40, 2008, in Russian.

[39] P. V. Krot, "Methods and equipment for measuring wear in the drive lines of rolling mills," *Metallurgical Processes and Equipment*, vol. 2, no. 12, pp. 45–53, 2008, in Russian.

[40] A. Yu. Putnoki, O. M. Klevtsov, A. A. Ermolenko et al., "Evaluation of operation of equipment at the rolling mill," *Stal'*, vol. 10, pp. 56–58, 2003, in Russian.

[41] P. V. Krot, K. V. Solovyov, V. V. Korennoy et al., "Monitoring system for mechanical loads of a hot rolling mill 1680 based on current loads of electric drives," *Collection of research papers of National Mining University*, vol. 5, no. 19, pp. 71–76, 2004, in Russian.

[42] Z. Cai, Y. Xu, and Z. Duan, "An alternative demodulation method using envelope-derivative operator for bearing fault diagnosis of the vibrating screen," *Journal of Vibration and Control*, vol. 24, no. 15, pp. 3249–3261, 2018.

[43] J. Liu, "A dynamic modelling method of a rotor-roller bearing-housing system with a localized fault including the additional excitation zone," *Journal of Sound and Vibration*, vol. 469, Article ID 115144, 2020.

[44] J. Liu, Z. Xu, L. Zhou, W. Yu, and Y. Shao, "A statistical feature investigation of the spalling propagation assessment for a ball bearing," *Mechanism and Machine Theory*, vol. 131, pp. 336–350, 2019.

[45] R. Zimroz, J. Obuchowski, and A. Wylomańska, "Vibration analysis of copper ore crushers used in mineral processing plant – problem of bearings damage detection in presence of heavy impulsive noise," in *Advances in Condition Monitoring of Machinery in Non-stationary Operations, CMMNO 2014, Applied Condition Monitoring*, F. Chaari, Ed., vol. 4, pp. 57–70, Springer, Cham, Switzerland, 2016.

[46] A. Wylomanska, R. Zimroz, and J. Janczura, "Identification and stochastic modelling of sources in copper ore crusher vibrations," *Journal of Physics: Conference Series*, vol. 628, Article ID 012125, 2015.

[47] A. Wylomanska, R. Zimroz, J. Janczura, and J. Obuchowski, "Impulsive noise cancellation method for copper ore crusher vibration signals enhancement," *IEEE Transactions on Industrial Electronics*, vol. 63, no. 9, pp. 5612–5621, 2016.

[48] J. Wodecki, A. Michalak, and R. Zimroz, "Optimal filter design with progressive genetic algorithm for local damage detection in rolling bearings," *Mechanical Systems and Signal Processing*, vol. 102, pp. 102–116, 2018.

[49] A. Michalak, J. Wodecki, A. Wyłomańska, and R. Zimroz, "Application of cointegration to vibration signal for local damage detection in gearboxes," *Applied Acoustics*, vol. 144, pp. 4–10, 2019.

[50] J. Obuchowski, R. Zimroz, and A. Wylomanska, "Identification of cyclic components in presence of non-Gaussian noise–application to crusher bearings damage detection," *Journal of Vibroengineering*, vol. 17, no. 3, pp. 1242–1252, 2015.

[51] L.-P. Peng, C.-s. Liu, B.-c. Song, J.-d. Wu, and S. Wang, "Improvement for design of beam structures in large vibrating screen considering bending and random vibration," *Journal of Central South University*, vol. 22, no. 9, pp. 3380–3388, 2015.

[52] V. S. Sorokin, "Vibrations of a nonlinear stochastic system with a varying mass under near resonant excitation," *Journal of Vibration and Control*, pp. 1–10, 2019.

[53] J. Detyna, "Stochastic models of particle distribution in separation processes," *Archives of Civil and Mechanical Engineering*, vol. 10, no. 1, pp. 15–26, 2010.

[54] P. V. Krot, "Nonlinear vibrations and backlashes diagnostics in the rolling mills drive trains," in *Proceedings of the 6th EUROMECH Nonlinear Dynamics Conference (ENOC 2008), IPME RAS*, pp. 360–366, St.Petersburg, Russia, June–July 2008.

[55] P. V. Krot, "Dynamics and diagnostics of the rolling mills drivelines with non-smooth stiffness characteristics," in *Proceedings of the 3rd International Conference on Nonlinear Dynamics (ND-KhPI2010)*, pp. 115–120, Kharkiv, Ukraine, September 2010.

[56] P. V. Krot and V. V. Korennoy, "Nonlinear effects in rolling mills dynamics," in *Proceedings of the 5th International Conference on Nonlinear Dynamics (ND-KhPI2016)*, pp. 117–124, Kharkiv, Ukraine, September 2016.

[57] P. V. Krot, "Statistical dynamics of the rolling mills," in *Proceedings of the IUTAM 2009 Symposium on the Vibration*

Analysis of Structures with Uncertainties, vol. 27, no. 4, pp. 429–442, St. Petersburg, Russia, July 2009.

[58] M. Trumic and N. Magdalinovic, "New model of screening kinetics," *Minerals Engineering*, vol. 24, no. 1, pp. 42–49, 2011.

[59] L. P. Peng, R. Fang, H. Feng, L. Zhang, W. Ma, and X. He, "A more accurate dynamic model for dual-side excitation large vibrating screens," *Journal of Vibration and Control*, vol. 20, pp. 858–871, 2018.

[60] C. G. Rodriguez, M. A. Moncada, E. E. Dufeu, and M. I. Razeto, "Nonlinear model of vibrating screen to determine permissible spring deterioration for proper separation," *Shock and Vibration*, vol. 2016, Article ID 4028583, 7 pages, 2016.

[61] G. Q. Lu, K. P. Xu, W. B. Peng, M. Ragulskis, and B. Wang, "Coupling dynamic stiffness identification of mechanical assembly with linear connection by the second indirect scheme of inverse substructuring analysis," *Vibroengineering Procedia*, vol. 20, pp. 24–29, 2018.

[62] Y. Liu, S. Suo, G. Meng, D. Shang, L. Bai, and J. Shi, "A theoretical rigid body model of vibrating screen for spring failure diagnosis," *Mathematics*, vol. 7, no. 246, 2019.

[63] Y. Liu, G. Meng, S. Suo et al., "Spring failure analysis of mining vibrating screens: numerical and experimental studies," *Applied Sciences*, vol. 9, p. 3224, 2019.

[64] C. Liu, L. Peng, and F. Li, "Survey of signal processing methods and research on vibrating screen fault diagnosis," in *Proceedings of the 2nd International Conference on Mechanic Automation and Control Engineering (MACE '11)*, pp. 1709–1712, IEEE, Hohhot, China, July 2011.

[65] L. Peng, C. Liu, and H. Wang, "Health identification for damping springs of large vibrating screen based on stiffness identification," *Journal of China Coal Society*, vol. 41, pp. 1568–1574, 2016, in Chinese.

[66] L.-p. Peng, C.-s. Liu, J. Li, and H. Wang, "Static-deformation based fault diagnosis for damping spring of large vibrating screen," *Journal of Central South University*, vol. 21, no. 4, pp. 1313–1321, 2014.

[67] Y.-Z. Jiang, K.-F. He, Y.-L Dong et al., "Influence of load weight on dynamic response of vibrating screen," *Shock and Vibration*, vol. 2019, Article ID 4232730, 8 pages, 2019.

[68] M. Moncada and C. G. Rodriguez, "Dynamic modeling of a vibrating screen considering the ore inertia and force of the ore over the screen calculated with discrete element method," *Shock and Vibration*, vol. 2018, Article ID 1714738, 13 pages, 2018.

[69] T. H. Mohamad and C. Nataraj, "An overview of PST for vibration based fault diagnostics in rotating machinery," *MATEC Web of Conferences*, vol. 211, Article ID 01004, 2018.

[70] M. Kowalski, "Phase mapping in the diagnosing of a turbojet engine," *Journal Of Theoretical And Applied Mechanics*, vol. 50, no. 4, pp. 913–921, 2012.

[71] W. J. Wang, J. Chen, X. K. Wu, and Z. T. Wu, "The application of some non-linear methods in rotating machinery fault diagnosis," *Mechanical Systems and Signal Processing*, vol. 15, no. 4, pp. 697–705, 2001.

[72] Y.-O. Jung and Y. Bae, "Analysis of fault diagnosis for current and vibration signals in pumps and motors using a reconstructed phase portrait," *The International Journal of Fuzzy Logic and Intelligent Systems*, vol. 15, no. 3, pp. 166–171, 2015.

[73] A. P. Bovsunovsky and O. Bovsunovsky, "Crack detection in beams by means of the driving force parameters variation at non-linear resonance vibrations," *Key Engineering Materials*, vol. 347, pp. 413–420, 2007.

[74] L. Gelman, S. Gorpinich, and C. Thompson, "Adaptive diagnosis of the bilinear mechanical systems," *Mechanical Systems and Signal Processing*, vol. 23, no. 5, pp. 1548–1553, 2009.

[75] L. Gelman, "Piecewise model and estimates of damping and natural frequency for a spur gear," *Mechanical Systems and Signal Processing*, vol. 21, no. 2, pp. 1192–1196, 2007.

[76] P. Fang, H. Peng, D. Changcheng et al., "Synchronous state of unbalanced rotors in a three-dimensional space and far-resonance system," *Proceedings of the Institution of Mechanical Engineers, Part E: Journal of Process Mechanical Engineering*, vol. 234, no. 1, pp. 108–122, 2020.

[77] X. Xiong, L. Niu, C. Gu, and Y. Wang, "Vibration characteristics of an inclined flip-flow screen panel in banana flip-flow screens," *Journal of Sound and Vibration*, vol. 411, pp. 108–128, 2017.

[78] R. Weron, "On the Chambers-Mallows-Stuck method for simulating skewed stable random variables," *Statistics & Probability Letters*, vol. 28, no. 2, pp. 165–171, 1996.

[79] G. Zak, A. Wyłomanska, and R. Zimroz, "Data-driven iterative vibration signal enhancement strategy using alpha-stable distribution," *Shock and Vibration*, vol. 2017, Article ID 3698370, 11 pages, 2017.